AD

TECHNICAL REPORT ARCCB-TR-01024

EROSION MODELING OF VENTED COMBUSTOR CANNON BORE MATERIALS

SAMUEL SOPOK

NOVEMBER 2001

US ARMY ARMAMENT RESEARCH,
DEVELOPMENT AND ENGINEERING CENTER
CLOSE COMBAT ARMAMENTS CENTER
BENÉT LABORATORIES
WATERVLIET, N.Y. 12189-4050

DISCLAIMER

The findings in this report are not to be construed as an official Department of the Army position unless so designated by other authorized documents.

The use of trade name(s) and/or manufacturer(s) does not constitute an official endorsement or approval.

DESTRUCTION NOTICE

For classified documents, follow the procedures in DoD 5200.22-M, Industrial Security Manual, Section II-19, or DoD 5200.1-R, Information Security Program Regulation, Chapter IX.

For unclassified, limited documents, destroy by any method that will prevent disclosure of contents or reconstruction of the document.

For unclassified, unlimited documents, destroy when the report is no longer needed. Do not return it to the originator.

REPORT DOCUMENTATION PAGE

Form Approved
OMB No. 0704-0188

1. AGENCY USE ONLY (Leave blank)	2. REPORT DATE	3. REPORT TYPE AND DATES COVERED
	November 2001	Final

4. TITLE AND SUBTITLE

EROSION MODELING OF VENTED COMBUSTOR CANNON BORE MATERIALS

5. FUNDING NUMBERS

AMCMS No. 6330.04.43A1.1

6. AUTHOR(S)

Samuel Sopok

7. PERFORMING ORGANIZATION NAME(S) AND ADDRESS(ES)

U.S. Army ARDEC
Benet Laboratories, AMSTA-AR-CCB-O
Watervliet, NY 12189-4050

8. PERFORMING ORGANIZATION REPORT NUMBER

ARCCB-TR-01024

9. SPONSORING / MONITORING AGENCY NAME(S) AND ADDRESS(ES)

U.S. Army ARDEC
Close Combat Armaments Center
Picatinny Arsenal, NJ 07806-5000

10. SPONSORING / MONITORING AGENCY REPORT NUMBER

11. SUPPLEMENTARY NOTES

Presented at the 35th AIAA Thermophysics Conference, Anaheim, CA, June 2001.
Published in proceedings of the conference.

12a. DISTRIBUTION / AVAILABILITY STATEMENT

Approved for public release; distribution unlimited.

12b. DISTRIBUTION CODE

13. ABSTRACT *(Maximum 200 words)*

Vented combustor experiments are often successful at providing relative erosion results, but these results are typically inconclusive when compared to other vented combustor experiments. As a result of this deficiency, a new method for successfully modeling erosion of vented combustor cannon bore materials has been developed. This modeling method, in conjunction with limited-scale firings, provides a cost effective means of comprehensively studying erosion of coated cannon bore materials. The method is derived from our very successful similar method for modeling coated cannon bore erosion of medium and large caliber gun systems. These system models are based on years of eroded cannon characterizations and erosion theory development. We have fired and modeled gun steel, chromium, tantalum, molybdenum, rhenium, and niobium cannon bore protection materials. Each of these material types has a different set of erosive degradation thresholds that are governed by the presence of a less-reducing (more-metal oxidizing), more-reducing (more-metal carburizing), or intermediate-reducing solid propellant combustion environment. Erosion modeling predictions are computed for these six materials at the various reducing combustion environment degrees. Our modeling results show that all of these materials, with the exception of chromium, have significant differences in their erosive thresholds/performance for our typical solid propellant combustion environment spectrum. The degree of these differences explains why these materials erode so differently at the more-metal carburizing and oxidizing solid propellant combustion environment extremes.

14. SUBJECT TERMS

Erosion Modeling, Vented Combustors, Cannon Bore Materials, Combustor Modeling, Gas/Wall Reaction Kinetics

15. NUMBER OF PAGES

17

16. PRICE CODE

17. SECURITY CLASSIFICATION OF REPORT	18. SECURITY CLASSIFICATION OF THIS PAGE	19. SECURITY CLASSIFICATION OF ABSTRACT	20. LIMITATION OF ABSTRACT
UNCLASSIFIED	UNCLASSIFIED	UNCLASSIFIED	UL

TABLE OF CONTENTS

Page

INTRODUCTION 1

COMPUTATIONAL AND EXPERIMENTAL METHODS 1

RESULTS AND DISCUSSION 2

REFERENCES 10

LIST OF ILLUSTRATIONS

1. 200-cc vented combustor 12

2. Reproducible vented combustor firings 12

3. Vented combustor magnifying borescope data 13

4. Vented combustor exposed substrate interface 13

5. Gas/wall oxidation rate 14

6. Vented combustor ring sample erosion 14

7. Flow chart of cannon/vented combustor coating erosion models 15

8. Summary of measured and calculated bore material degradation thresholds for solid propellant spectrum 15

9. Calculated initial erosive thresholds 16

INTRODUCTION

A practical thermal-chemical vented combustor erosion model is described herein. It was a natural extension of our thermal-chemical-mechanical erosion model for medium and large caliber cannons (refs 1-5). Benet Laboratories has had the U.S. Army mission for characterizing eroded cannons for many years. These characterizations have allowed us to develop erosion theories that we have repeatedly verified for a broad spectrum of gun systems (refs 1-7). Both of these erosion model types require a systems approach where variations in bore material type (coating, substrate, and axial position), charge type (propellant, loading density, and ablatives), and/or projectile type (round type and rounds fired) are considered. Most commonly, these erosion calculations are made for either a constant bore material type with varied charge types or a varied bore material type with a constant charge type.

Our calculations of erosion between various vented combustor system samples depend on:

- Erosive gas/wall combustion chemistry
- Degree of achievement of bore material degradation thresholds (measured wall temperature onsets)
- Time spent above these bore material degradation thresholds

Without modeling, vented combustor experiments are often successful at simulating relative erosion results, but are typically inconclusive at simulating absolute erosion results. Our vented combustor erosion modeling can do absolute erosion predictions because it accounts for variations in geometry, cannon bore material type, charge type, and projectile types.

COMPUTATIONAL AND EXPERIMENTAL METHODS

Our vented combustor and cannon erosion models consist of a number of interactively linked codes and are used to predict wall temperature profiles and erosion profiles (ref 1-5). The overall erosion code includes the following:

- CCET thermochemistry cannon code (refs 1-5,8)
- XNOVAKTC interior ballistics code (refs 1-5,9)
- MABL boundary layer cannon code (refs 1-5,10)
- MACE thermal-erosion cannon code (refs 1-5,11)

These erosion predictions are guided and calibrated by substantial firing data and fired specimen analyses. Our vented combustor modeling approach requires a burst disk and a pseudo-projectile with at least minor bore resistance.

A borrowed 200-cc vented combustor (ref 12) was fired at our Building 112 range in 1994 and then at an ARDEC range in Dover, NJ, in the following years. Each safety office required a detailed description of each firing test that was supported by modeling calculations. This combustor used electric match ignition, 0.17-g/cc IMR4895 baseline solid propellant, numerous other erosive solid propellants, and burst disks that achieved/failed at 30 kpsi. Cased igniters/charges were more reproducible than their cellophane-bagged counterparts. For the baseline IMR4895 solid propellant firings, the BLAKE composition was NC1315 at 88.8%, DNT at 7.2%, DPA at 0.6%, KS at 0.9%, H_2O at 1.0%, and ETOH at 1.5% (ref 13), which produced a 2830°K peak flame temperature. Pressure transducer data were captured, amplified, and input through an IEEE-488 interface bus controller to a data-reduction computer. The models were calibrated by pressure gages, thermocouples, and gas/wall thermal, metallurgical, and chemical characterizations.

RESULTS AND DISCUSSION

We developed vented combustor erosion testers for screening, assessing, and optimizing gun bore protection materials. Their environment approximates specific gun system core flow and combustion products. Most of these combustors have associated erosion models. Progressively increasing the energies and densities of charges requires increased erosion-resistant cannon bore protection materials. Vented combustor cannon bore protection material samples include medium and large caliber plates, rings, and ring sections. Cannon bore protection material types include gun steel, pure chromium, high contraction chromium, low contraction chromium, pure tantalum, pure molybdenum, pure rhenium, and pure niobium (columbium).

From 1994 to the present, Benet Laboratories and ARDEC have conducted vented combustor firings to assess cannon bore protection materials (ref 14). Figure 1 depicts a 200-cc vented combustor, and Figure 2 shows its reproducible baseline IMR4895 solid propellant firings.

Figure 3 shows typical nondestructive magnifying borescope substrate exposure and erosion data from monitoring a vented combustor sample throughout its life at the mid-sample position. Substrate exposure is based on crack/pit frequency, coating shrinkage and contraction, and crack/pit widths. This technique is used due to the lack of a thermal-mechanical crack/pit model.

The use of magnifying borescope substrate exposure measurements allows modeling of the conductive and convective exposed gun steel interface temperatures at the base of coating cracks/pits. Figure 4 depicts typical maximum values of exposed substrate interface temperatures as a function of coating crack/pit width throughout its life at the vented combustor mid-sample position. Based on these exposed gun steel interface temperatures, we thermally, metallurgically, and thermochemically use the model to degrade the exposed gun steel substrate interface through the coating cracks/pits, producing coating platelet spallation and subsequent exposed gun steel gas wash-to-condemnation.

A gas/wall kinetic rate characterization technique is used to study coating and substrate steel degradation thresholds and reaction rates as a function of temperature, pressure, and time. This technique determines degradation thresholds of bore coating and substrate materials for their transformation, carburization, oxidation-scale, other reactions, oxide melting, and metal melting thresholds. Figure 5 shows typical normalized gas/wall coating and substrate steel oxidation rate data as a function of wall temperature at the vented combustor mid-sample position. Our main erosion-related thrust for implementing vented combustors in 1994 was to measure gas/wall kinetic rate functions of bore protection materials.

Figure 6 shows a typical ring sample erosion throughout its life at the vented combustor mid-sample position. Sample types include gun steel and 0.002-inch high contraction chromium plated steel. This vented combustor was better than an order-of-magnitude more erosive than a typical gun system. Ideally, vented combustor firing intensity should be similar to gun system firing intensity in order to simulate its correct cannon erosion mechanisms for a given propellant.

Figure 7 presents a flow chart of the vented combustor/cannon coating erosion models. The various codes, their inputs, and their outputs have respective boxes with solid borders, fine-dashed borders, and coarse-dashed borders.

There are three main reasons why vented combustor experiments have only been successful at simulating relative erosion results. The first reason is that varying loading density of a given charge type will affect the lack of achievement or degree of achievement of the several degradation thresholds for each bore material type. Variations in loading density of a given charge type will affect its maximum pressure and velocity with little effect on flame temperature.

The second reason is that varying gas/wall combustion chemistries (single or multiple propellant types) will affect the lack of achievement or degree of achievement of the several degradation thresholds for each bore material type. Single propellant gas/wall combustion chemistry variations will affect gas/wall degrading and reacting species, gas/wall degradation and reaction enthalpies, but have little effect on flame temperature. Multiple propellant gas/wall combustion chemistry variations will affect gas/wall degrading and reacting species, gas/wall degradation and reaction enthalpies, and flame temperature.

The third reason is that each bore material type has a different set of erosive bore material degradation thresholds. For each material, the degree of combustor charge type conditions affects the lack of achievement or degree of achievement of its lowest erosive threshold. With relatively mild gun system conditions using typical solid propellants, some bore material types achieve their lowest erosive bore material degradation thresholds, such as the measurable sublimation of pure rhenium at about 670°K or the measurable flaking oxidation of pure niobium (columbium), at about 680°K. With relatively moderate gun system conditions using typical solid propellants, other bore material types achieve their lowest erosive bore material degradation thresholds such as the measurable flaking oxidation of gun steel (mostly iron) at about 1050°K and the measurable sublimation of pure molybdenum at about 1080°K. Even with relatively severe gun system conditions using typical solid propellants, other bore material types do not achieve their lowest erosive bore material degradation thresholds due to oxidation

passivation (chromium and tantalum), but they form a network of radial cracks due to shrinkage/thermal shock allowing the exposed gun steel substrate to erode. This leads to coating spallation, pitting, and increased surface roughness that further increases heat transfer, turbulence, boundary layer separation, spallation, and pitting.

Pure molybdenum is the classic example of different vented combustor tests producing a broad range of erosion-resistant results. The lack of achievement or degree of achievement of the measurable sublimation of pure molybdenum at about 1080°K determines its erosion-related outcome.

Based on their associated erosion models, gun system and vented combustor system erosion comparisons can be made for the same bore material types and charge types. Quantitative calculations of erosion between the vented combustor samples and the various positions on the cannon bore depend on erosive gas/wall combustion chemistry, bore material degradation thresholds (measured wall temperature onsets), and time spent above these bore material degradation thresholds. By varying the vented combustor propellant loading density, vented combustor sample erosion can be made to correspond to different eroded positions on the cannon bore.

All of the above cannon system and vented combustor system erosion modeling efforts start with interior ballistic and thermochemical modeling. These codes allow for the simultaneous calculation of pressure, temperature, and velocity core flow conditions at the desired bore or sample position as a function of time. The core flow and thermochemical output data allow for the subsequent boundary layer calculation. Then the core flow, thermochemical, and boundary layer output data allow for the thermal and erosion calculation.

Figure 8 gives a summary of bore material degradation thresholds (measured and calculated wall temperature onsets) based on a spectrum of typical solid propellants. These six bore material types include gun steel, pure chromium, pure tantalum, pure molybdenum, pure rhenium, and pure niobium (columbium). Their thresholds include measurable transformations, reactions, reaction product melting points, and metal melting points. In the following paragraphs, each of these bore material types will be discussed in greater detail based on typical solid propellants.

Gun steel (mostly iron) bore and substrate degradation of surfaces, cracks, pits, and interfaces is computed by the area under a temperature-time curve above a given degradation threshold such as:

- Measurable 1000°K transformation onset of steel, which may induce heat checking
- Measurable 1050°K diffusion onset of carbon into the steel
- Measurable 1050°K accelerated flaking scale-type oxidation onset (trace onset at 670°K) of iron by oxygen forming iron oxide (FeO)
- Measurable 1270°K accelerated flaking scale-type oxidation onset of iron by sulfur forming iron sulfide (FeS)
- Measurable 1420°K white layer eutectic melting point onset of iron carbide
- Measurable 1470°K melting point onset of iron sulfide

- Measurable 1640°K melting point onset of iron oxide
- Measurable 1700°K melting point onset of gun steel
- Measurable 2110°K melting point onset of iron carbide

Although chromium plate for cannon bores is not pure, the following values are quite close to pure chromium despite variation in cannon chromium plate types. Chromium coating degradation of surfaces, cracks, pits, and interfaces is computed by the area under a temperature-time curve above a given degradation threshold such as:

- Measurable 2000°K accelerated oxidation onset (trace onset at 1960°K) and passivation of chromium by oxygen forming Cr2O3
- Measurable 2110°K transformation onset of chromium
- Measurable 2130°K melting point onset of chromium
- Measurable 2540°K melting point onset of Cr2O3
- Measurable 4070°K melting point onset of Cr3C2

Chromium forms an interfacial intermetallic with iron above 1050°K, and is subject to intergranular corrosion above 1090°K. It is also susceptible to hydrogen, nitrogen, and oxygen embrittlement above 400°K.

Pure tantalum coating degradation of surfaces, cracks, pits, and interfaces is computed by the area under a temperature-time curve above a given degradation threshold such as:

- Measurable 720°K accelerated oxidation onset (trace onset at 570°K) and passivation of tantalum by oxygen forming Ta2O5
- Measurable 2150°K melting point onset of Ta2O5
- Measurable 3270°K melting point onset of tantalum
- Measurable 4150°K melting point onset of TaC2

Tantalum forms an interfacial intermetallic with iron above 1050°K, and is susceptible to oxygen, hydrogen, and nitrogen embrittlement above 400°K.

Pure molybdenum coating degradation of surfaces, cracks, pits, and interfaces is computed by the area under a temperature-time curve above a given degradation threshold such as:

- Measurable 1080°K accelerated oxidation onset (trace onset at 1030°K) and sublimation of molybdenum by oxygen forming MoO3 (oxide evaporates as formed)
- Measurable 1080°K melting point onset of MoO3 solid that is the same as the measurable molybdenum oxidation onset due to sublimation
- Measurable 2470°K melting point onset of MoC2
- Measurable 2890°K melting point onset of molybdenum

Pure rhenium coating degradation of surfaces, cracks, pits, and interfaces is computed by the area under a temperature-time curve above a given degradation threshold such as:

- Measurable 670°K accelerated oxidation onset (trace onset at 420°K) and sublimation of rhenium by oxygen forming Re2O7 (oxide evaporates as formed)
- Measurable 670°K melting point onset of Re2O7 solid that is the same as the measurable rhenium oxidation onset due to sublimation
- Measurable 2700°K melting point onset of Re4C3
- Measurable 3450°K melting point onset of rhenium

Pure niobium (also columbium or Cb) coating degradation of surfaces, cracks, pits, and interfaces is computed by the area under a temperature-time curve above a given degradation threshold such as:

- Measurable 680°K accelerated flaking scale-type oxidation onset (trace onset at 300°K) of niobium by oxygen forming Nb2O5
- Measurable 1760°K melting point onset of Nb2O5
- Measurable 2740°K melting point onset of niobium
- Measurable 4070°K melting point onset of NbC

The measurable 680°K accelerated flaking scale-type oxidation onset of niobium by oxygen, forming Nb2O5, is due to nucleation and growth of the porous oxide that keeps a continuously refreshed surface of niobium exposed to corrosion. Niobium forms an interfacial intermetallic with iron above 1050°K, and is susceptible to oxygen, hydrogen, and nitrogen embrittlement above 400°K.

The vented combustor or gun system reaction energy is all the energy for future reactions and melting. This reaction energy is enthalpy driven and highly dependent on all chemical species present, reactions present, and their chemical kinetics. A given propellant chemistry type with a constant loading density may be mainly oxidizing to some wall materials, while mainly carburizing to other wall materials depending on the gas/wall temperatures and chemical species present.

Erosion predictions of these six bore protection materials are computed for numerous typical less-metal reducing (more-oxidizing) solid propellant combustion environments and more-metal reducing (more-carburizing) solid propellant combustion environments. The more-oxidizing propellant types typically have a higher flame temperature with more erosive combustion species and a minor level of carburization. The more-carburizing propellant types typically have a lower flame temperature with less erosive combustion species and a minor level of oxidation. It should be noted that the more-oxidizing and more-carburizing solid propellant types are at the end of a spectrum of oxidation and carburization combinations, which contain a range of flame temperatures and gas/wall combustion chemistry. Figure 8 shows that some bore material types, such as gun steel, may be nearly equal in their oxidation and carburization levels.

Calculated initial erosive threshold predictions for typical more-metal oxidizing (less-reducing) solid propellant types are summarized in Figure 9. These calculations tend to represent the solid propellant metal oxidation boundary or extreme for this study.

For the more-metal oxidizing solid propellant types, pure rhenium has the least erosion resistance. This is due to its accelerated oxidation/sublimation product Re2O7 formed at about 670°K. A trace of its dominant carbide product Re4C3 is still measurable. Rhenium alloys with iridium are much more oxidation and erosion-resistant than pure rhenium.

Pure niobium (columbium) has the next least metal oxidative erosion resistance due to its accelerated flaking scale oxidation product Nb2O5 formed at about 680°K. This oxide melts at about 1760°K. This oxide scale is porous and flakes exposing a continuously refreshed surface of metal to corrosion. A trace of its dominant carbide product NbC is still measurable. Oxidation-resistant niobium alloys have better erosion resistance than pure niobium. At high temperatures, pure niobium is susceptible to hydrogen, nitrogen, and oxygen embrittlement and forms intermetallics with iron. Hydrogen is available in lesser amounts for this fully oxidizing case, and its absorption is diminished.

Pure molybdenum has the next least metal oxidative erosion resistance due to its accelerated oxidation/sublimation product MoO3 formed at about 1080°K. A trace of its dominant carbide product Mo2C is still measurable. Oxidation-resistant molybdenum alloys have better erosion resistance than pure molybdenum.

Gun steel (mostly iron) has the next least metal oxidative erosion resistance due to its accelerated flaking scale oxidation products FeO and FeS formed at about 1050°K and 1270°K, respectively. These oxidation products melt at about 1640°K and 1470°K. The 1050°K formation of FeO is less damaging than the oxidations coupled with sublimations mentioned above. This oxide scale is porous and flakes exposing a continuously refreshed surface of metal to corrosion. A trace of its dominant carbide product Fe3C is still measurable. Gun steel transforms at about 1000°K.

Although chromium plate for cannon bores is not pure, the following values are quite close to pure chromium, despite variation in cannon chromium plate types. This chromium has the next least metal oxidative erosion resistance due to its metal melting point at about 2130°K. It also forms a nondamaging, accelerated oxidation product Cr2O3 at about 2000°K that melts at about 2540°K. This oxide scale is passivated and does not expose a continuously refreshed surface of metal to corrosion. A trace of its dominant carbide product Cr3C2 is still measurable. At high temperatures, pure chromium is susceptible to hydrogen, nitrogen, and oxygen embrittlement and forms intermetallics with iron.

Pure tantalum has the most metal oxidative erosion resistance due to its oxidation product Ta2O5 melting point at about 2150°K. It forms this nondamaging, accelerated oxidation product Ta2O5 at about 720°K. The oxide scale is passivated and does not expose a continuously refreshed surface of metal to corrosion. A trace of its dominant carbide product TaC2 is still measurable. At high temperatures, pure tantalum is susceptible to hydrogen, nitrogen, and oxygen embrittlement and forms intermetallics with iron. Tantalum has the potential at high

temperatures to absorb up to 700 times its own volume of hydrogen, which can severely embrittle the metal. Hydrogen is available in lesser amounts for this fully oxidizing case, and its absorption is diminished.

Similar calculated initial erosive threshold predictions for typical more-metal carburizing (more-reducing) solid propellant types are also summarized in Figure 9. These calculations tend to represent the solid propellant metal carburization boundary or extreme for this study.

For the more-metal carburizing solid propellant types, pure gun steel (mostly iron) has the least erosion resistance. This is due to its carbide product Fe3C white layer eutectic melting point at about 1420°K. It begins forming this carbide product Fe3C at about 1050°K. Traces of its dominant oxidation products FeO and FeS are still measurable. Gun steel transforms at about 1000°K.

Although chromium plate for cannon bores is not pure, the following values are quite close to pure chromium despite variation in cannon chromium plate types. This chromium has the next least metal carburization erosion resistance due to its metal melting point at about 2130°K. A trace of its dominant oxide product Cr2O3 is still measurable. At high temperatures, pure chromium is susceptible to hydrogen, nitrogen, and oxygen embrittlement and forms intermetallics with iron.

Pure molybdenum has the next least metal carburization erosion resistance due to its carbide product Mo2C melting point at about 2470°K. A trace of its dominant oxide product MoO3 is still measurable.

Pure rhenium has the next least metal carburization erosion resistance due to its carbide product Re4C3 melting point at about 2700°K. A trace of its dominant oxide product Re2O7 is still measurable.

Pure niobium (columbium) has the next least metal carburization erosion resistance due to its metal melting point at about 2740°K. A trace of its dominant oxide product Nb2O5 is still measurable. At high temperatures, pure niobium is susceptible to hydrogen, nitrogen, and oxygen embrittlement and forms intermetallics with iron. Hydrogen is available in large amounts for this fully carburizing case, and its absorption and embrittling effect are significant. Free and/or loosely bound oxygen is available only in trace amounts for this fully carburizing case, and its absorption is limited.

Pure tantalum has the most metal carburization erosion resistance due to its metal melting point at about 3270°K. A trace of its dominant oxide product Ta2O5 is still measurable. At high temperatures, pure tantalum is susceptible to hydrogen, nitrogen, and oxygen embrittlement and forms intermetallics with iron. Tantalum has the potential at high temperatures to absorb up to 700 times its own volume of hydrogen, which can severely embrittle the metal. Hydrogen is available in large amounts for this fully carburizing case, and its absorption and embrittling effects are significant. Free and/or loosely bound oxygen is available only in trace amounts for this fully carburizing case, and its absorption is limited.

Propellant composition, propellant loading density, and combustor (or gun) geometry determine the time and position-dependent combustion gas pressures, temperatures, velocities, and high-energy chemical combustion gas species/radicals produced. These resultant combustion gas features determine the time and position-dependent wall heating and gas/metal wall chemical reactions.

The various erosive thresholds for combustion gas degradations and reactions of these metal walls depend on the wall temperatures, as well as the types and amounts of high-energy metal carburizing and oxidizing combustion gas chemical species present.

Very high-energy propellant components have higher-energy bonds within their molecules. If all else is equal, increasing the percentage of these very high-energy propellant components tends to increase erosion of traditional gun bore wall materials.

A number of conclusions can be drawn for each metal in Figure 9 based on their initial erosive threshold ranges for their more-metal oxidizing and carburizing solid propellant types. Chromium has no variation between its initial erosive threshold metal oxidation and carburization extremes. Gun steel has a small variation between its initial erosive threshold metal oxidation and carburization extremes. Tantalum and molybdenum have moderate variations between their initial erosive threshold metal oxidation and carburization extremes. Rhenium and niobium (columbium) have large variations between their initial erosive threshold metal oxidation and carburization extremes. If everything else is equal, modeling predictions indicate that differences between a metal's initial erosive thresholds due to its metal oxidation and carburization solid propellant extremes produce similar variations in erosion resistance. Variations in degree/type of solid propellant reducing environment explain why a material's erosion resistance may vary from one vented combustor experiment to another. Ideally, vented combustor firing intensity should be similar to gun system firing intensity in order to simulate its correct cannon erosion mechanisms for a given propellant.

Also, for a given metal, oxidation and carburization embrittlement variation results in large differences in erosion resistance. This is due to variations in radial crack density and contraction that induce crack widening and expose the gun steel substrate to the corrosive combustion gases.

In 1999, we developed a robust time-dependent gun tube boundary layer (GTBL) code (ref 15) to complement and eventually replace our current steady-state gun tube mass addition boundary layer (MABL) code (ref 10). In that same year, when conventional interior ballistic models failed us, we successfully began using the GTBL code for future combat system rarefaction wave gun (RAVEN) and associated vented combustor systems. In these RAVEN systems, high-velocity combustion gases exit both a breech venting nozzle for recoil reduction, as well as the conventional muzzle venting after projectile exit (ref 16). Our RAVEN modeling efforts make it possible to reject design configurations without full-scale firing tests, thus producing significant savings.

REFERENCES

1. Dunn, S., Sopok, S., Coats, D., O'Hara, P., Nickerson, G., and Pflegl, G., "Unified Computer Model for Predicting Thermochemical Erosion in Gun Barrels," *Proceedings of 31st AIAA Joint Propulsion Conference*, San Diego, CA, July 1995; Also, Sopok, S., Dunn, S., Coats, D., O'Hara, P., and Pflegl, G., "Unified Computer Model for Predicting Thermochemical Erosion in Gun Barrels," *AIAA Journal of Propulsion and Power*, Volume 15, Number 4, July 1999.

2. Sopok, S., O'Hara, P., Pflegl, G., Dunn, S., and Coats, D., "Thermochemical Erosion Modeling of M242 Gun Systems," *Proceedings of 8th U.S. Army Symposium on Gun Dynamics*, Newport, RI, May 1996.

3. Sopok, S., O'Hara, P., Vottis, P., Pflegl, G., Rickard, C., and Loomis, R., "Erosion Modeling of the 120-mm M256/M829A2 Gun System," *Proceedings of 32nd ADPA Gun and Ammunition Technical Meeting*, San Diego, CA, April 1997.

4. Sopok S., "Cannon Coating Erosion Model with Updated M829E3 Example," *Proceedings of 36th AIAA Joint Propulsion Conference*, Huntsville, AL, June 2000.

5. Sopok, S., and Fleszar, M., "Ablative Erosion Model for the M256/M829E3 Gun System," *Proceedings of 37th JANNAF Combustion Meeting*, Monterey, CA, November 2000.

6. Thornton, P., Senick, J., Underwood, J., Sopok, S., and Cox, J., "LP Gun No.2 Materials/ Failure Analysis," U.S. Army ARDEC Special Publication SP92-1, Watervliet, NY, 1992.

7. Capsimalis, G., Cox, J., O'Hara, P., Witherell, M., Sopok, S., Underwood, J., Pflegl, G., and Cote, P., "M242/ M919 Multi-Disciplinary Analyses," U.S. Army ARDEC Special Publication SP92-2, Watervliet, NY, 1992.

8. Coats, D., Dunn, S., and Sopok, S., "A New Chemical Equilibrium Code with Compressibility Effects (CCET)," *Proceedings of 33rd JANNAF Combustion Meeting*, Monterey, CA, October 1996.

9. Gough, P., "The XNOVAKTC Code," Paul Gough Associates, Portsmouth, NH, U.S. Army BRL-CR-627, February 1990.

10. Levine, J., "Transpiration and Film Cooling Boundary Layer Computer Program (MABL) - Numerical Solution of the Turbulent Boundary Layer Equations with Equilibrium Chemistry," NASA Marshall N72-19312, Huntsville, AL, June 1971.

11. Dunn, S., "Materials Ablation Conduction Erosion Program (MACE)," Software and Engineering Associates, Inc., Carson City, NV, June 1989.

12. Bracuti, Art, Dr., private communications on borrowed combustor, U.S. Army ARDEC, Dover, NJ, 1994.

13. Werner, Larry, private communications on propellants, IMR Power Company, Virginia Beach, VA, and Plattsburgh, NY, 1994.

14. Sopok, S., Pflegl, G., O'Hara, P., Cipollo, M., Keating, J., and Weber, P., "Vented Combustor Firings to Assess Cannon Bore Protection Materials," Memorandum Report, Benet Laboratories, Watervliet, NY, 1994.

15. Dunn, S., Coats, D., and Sopok, S., "Gun Tube Boundary Layer Code (GTBL)," Software and Engineering Associates, Inc., Carson City, NV, 1999.

16. Kathe, E., Dillon, R., Sopok, S., Witherell, M., Dunn S., and Coats, D., "Rarefaction Wave Gun Propulsion," *Proceedings of 37th JANNAF Combustion Meeting*, Monterey, CA, November 2000.

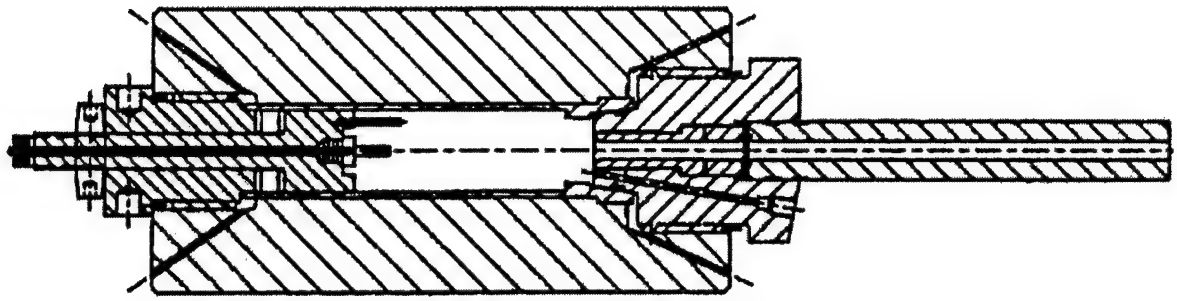

Figure 1. 200-cc vented combustor.

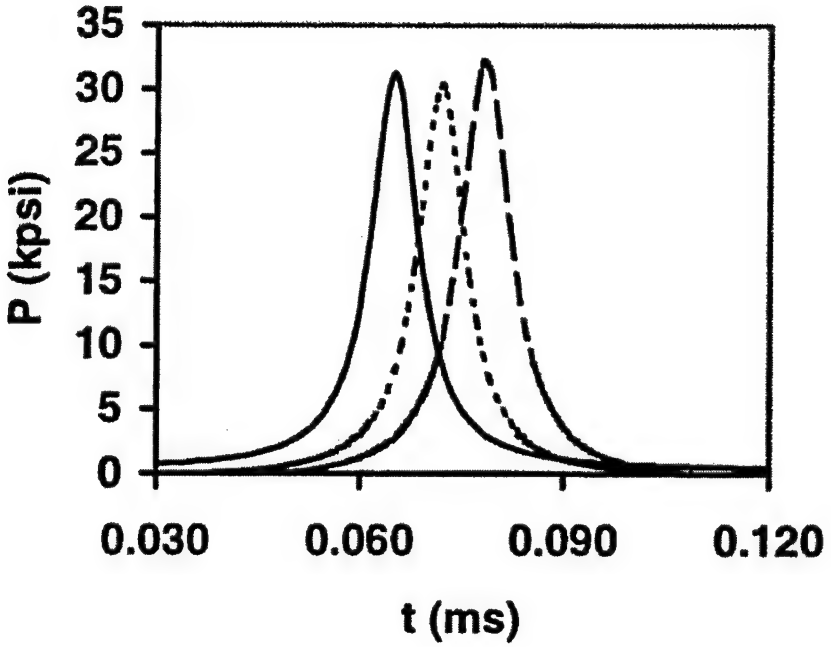

Figure 2. Reproducible vented combustor firings.

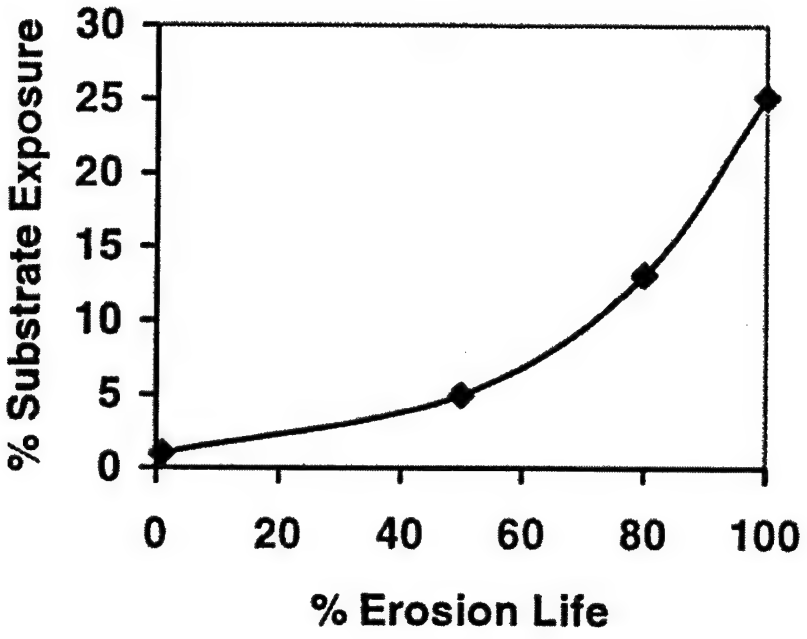

Figure 3. Vented combustor magnifying borescope data.

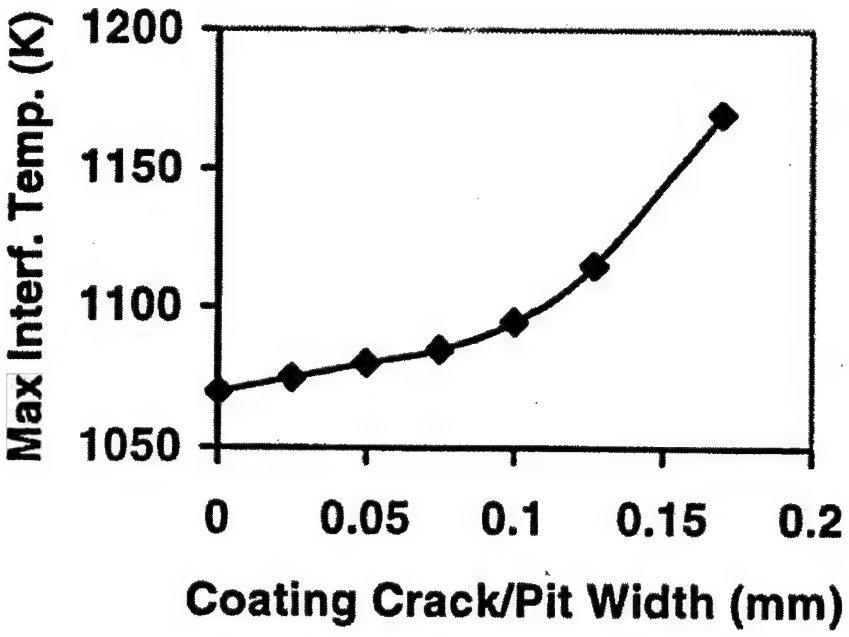

Figure 4. Vented combustor exposed substrate interface.

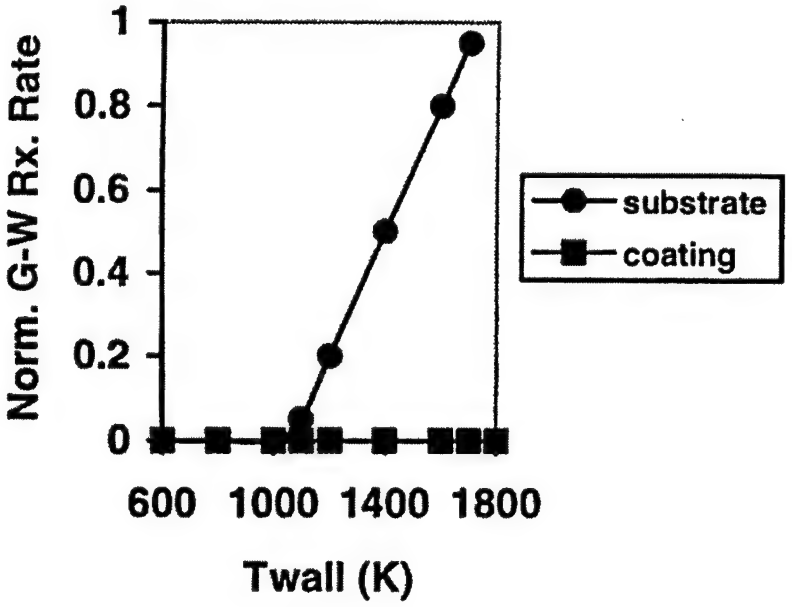

Figure 5. Gas/wall oxidation rate.

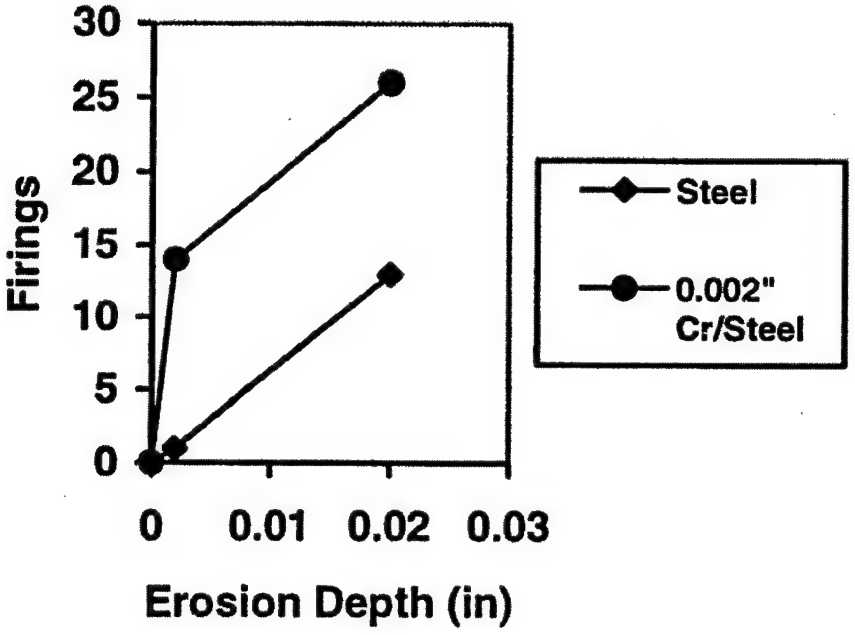

Figure 6. Vented combustor ring sample erosion.

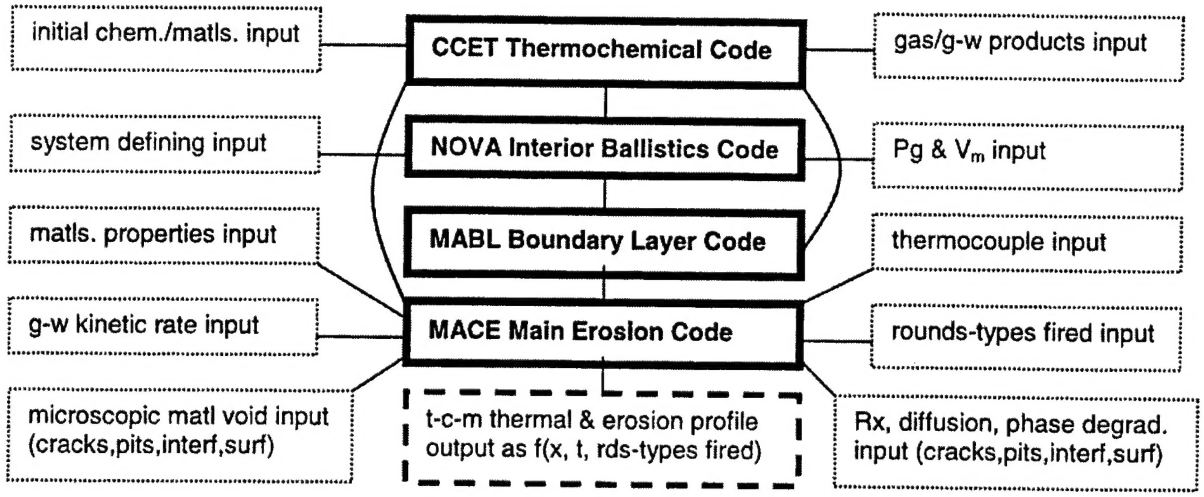

Figure 7. Flow chart of cannon/vented combustor coating erosion models.

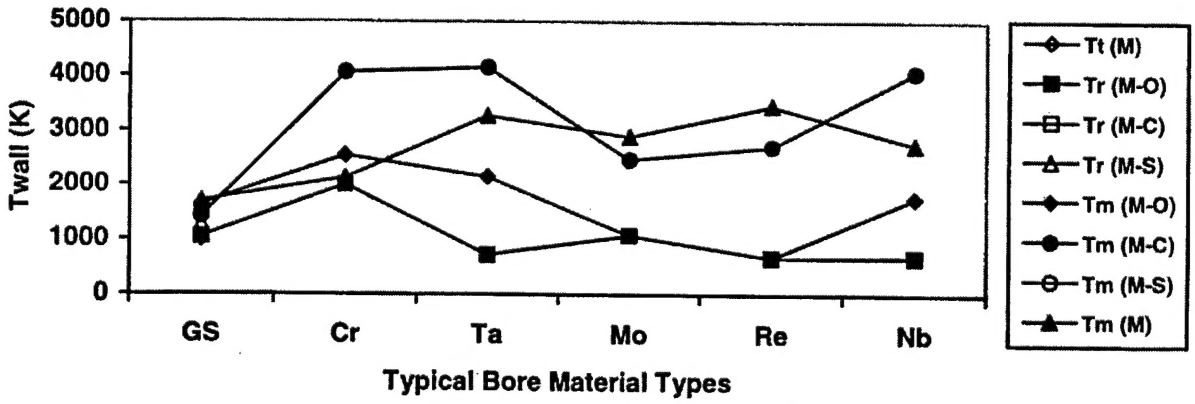

Figure 8. Summary of measured and calculated bore material degradation thresholds for solid propellant spectrum.

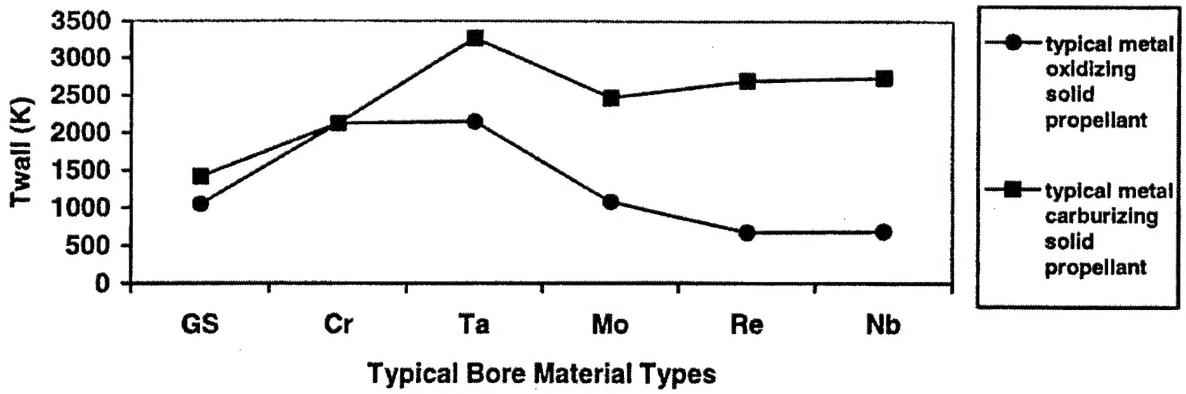

Figure 9. Calculated initial erosive thresholds.

TECHNICAL REPORT INTERNAL DISTRIBUTION LIST

	NO. OF COPIES
TECHNICAL LIBRARY ATTN: AMSTA-AR-CCB-O	5
TECHNICAL PUBLICATIONS & EDITING SECTION ATTN: AMSTA-AR-CCB-O	3
OPERATIONS DIRECTORATE ATTN: SIOWV-ODP-P	1
DIRECTOR, PROCUREMENT & CONTRACTING DIRECTORATE ATTN: SIOWV-PP	1
DIRECTOR, PRODUCT ASSURANCE & TEST DIRECTORATE ATTN: SIOWV-QA	1

NOTE: PLEASE NOTIFY DIRECTOR, BENÉT LABORATORIES, ATTN: AMSTA-AR-CCB-O OF ADDRESS CHANGES.

TECHNICAL REPORT EXTERNAL DISTRIBUTION LIST

	NO. OF COPIES
DEFENSE TECHNICAL INFO CENTER ATTN: DTIC-OCA (ACQUISITIONS) 8725 JOHN J. KINGMAN ROAD STE 0944 FT. BELVOIR, VA 22060-6218	2
COMMANDER U.S. ARMY ARDEC ATTN: AMSTA-AR-WEE, BLDG. 3022 AMSTA-AR-AET-O, BLDG. 183 AMSTA-AR-FSA, BLDG. 61 AMSTA-AR-FSX AMSTA-AR-FSA-M, BLDG. 61 SO AMSTA-AR-WEL-TL, BLDG. 59 PICATINNY ARSENAL, NJ 07806-5000	 1 1 1 1 1 2
DIRECTOR U.S. ARMY RESEARCH LABORATORY ATTN: AMSRL-DD-T, BLDG. 305 ABERDEEN PROVING GROUND, MD 21005-5066	 1
DIRECTOR U.S. ARMY RESEARCH LABORATORY ATTN: AMSRL-WM-MB (DR. B. BURNS) ABERDEEN PROVING GROUND, MD 21005-5066	 1
COMMANDER U.S. ARMY RESEARCH OFFICE ATTN: TECHNICAL LIBRARIAN P.O. BOX 12211 4300 S. MIAMI BOULEVARD RESEARCH TRIANGLE PARK, NC 27709-2211	 1
COMMANDER ROCK ISLAND ARSENAL ATTN: SIORI-SEM-L ROCK ISLAND, IL 61299-5001	 1
COMMANDER U.S. ARMY TANK-AUTMV R&D COMMAND ATTN: AMSTA-DDL (TECH LIBRARY) WARREN, MI 48397-5000	 1
COMMANDER U.S. MILITARY ACADEMY ATTN: DEPT OF CIVIL & MECH ENGR WEST POINT, NY 10966-1792	 1
U.S. ARMY AVIATION AND MISSILE COM REDSTONE SCIENTIFIC INFO CENTER ATTN: AMSAM-RD-OB-R (DOCUMENTS) REDSTONE ARSENAL, AL 35898-5000	 2
COMMANDER U.S. ARMY FOREIGN SCI & TECH CENTER ATTN: DRXST-SD 220 7TH STREET, N.E. CHARLOTTESVILLE, VA 22901	 1

NOTE: PLEASE NOTIFY COMMANDER, ARMAMENT RESEARCH, DEVELOPMENT, AND ENGINEERING CENTER, BENÉT LABORATORIES, CCAC, U.S. ARMY TANK-AUTOMOTIVE AND ARMAMENTS COMMAND, AMSTA-AR-CCB-O, WATERVLIET, NY 12189-4050 OF ADDRESS CHANGES.